One-dimensional maps with two discontinuity points and three linear branches: mathematical lessons for understanding the dynamics of financial markets

**Fabio Tramontana · Frank Westerhoff ·
Laura Gardini**

Abstract   We develop a simple financial market model with heterogeneous interacting speculators. The dynamics of our model is driven by a one-dimensional discontinuous piecewise linear map, having two discontinuity points and three linear branches. On the one hand, we study this map analytically and numerically to advance our knowledge about such dynamical systems. In particular, not much is known about discontinuous maps involving three branches. On the other hand, we seek to improve our understanding of the functioning of financial markets. We find, for instance, that such maps can generate complex bull and bear market dynamics.

1 Introduction

Day and Huang (1990) published their seminal bull and bear market model to explain the complex dynamics of financial markets. In their model, there are three types of market participants. Chartists buy (sell) assets when they perceive a bull (bear) market

F. Tramontana (✉)
Department of Economics and Management, University of Pavia, Pavia, Italy
e-mail: fabio.tramontana@unipv.it

F. Westerhoff
Department of Economics, University of Bamberg, Bamberg, Germany
e-mail: frank.westerhoff@uni-bamberg.de

L. Gardini
Department of Economics, Society and Politics, University of Urbino, Urbino, Italy
e-mail: laura.gardini@uniurb.it

and fundamentalists buy (sell) when the market is undervalued (overvalued). The third player is the market maker who adjusts prices with respect to the chartists' and fundamentalists' excess demand. As it turns out, the (nonlinear) model of Day and Huang is able to generate intricate price dynamics where complex bull market dynamics erratically alternate with complex bear market dynamics. This contribution was indeed seminal—it triggered hundreds of follow-up papers, of which some are surveyed in Chiarella et al. (2009); Hommes and Wagener (2009); Lux (2009) and Westerhoff (2009).

In 1993, Huang and Day (1993) developed a piecewise linear version of their original model. Due to the piecewise linear shape of their model, certain new insights into the properties and dynamics of their model were gained. Since then, only a few piecewise linear models have been proposed. The few exceptions include, for instance, Huang et al. (2010) and Tramontana et al. (2010). This is rather surprising—after all, piecewise linear models may offer novel interesting results about how financial markets function. One reason for this lack of development may have been that the mathematical tools, which are obviously necessary to study such systems, were rather limited. Therefore, the recent contributions in this area usually do not only aim at improving our understanding of financial markets but also at advancing our knowledge about how to deal with piecewise linear maps.

This is also true in our case. We develop a simple financial market model in the tradition of Day and Huang (1990) and Huang and Day (1993). Within our model, there are four types of speculators. Type 1 and type 2 chartists believe in the persistence of bull and bear markets; type 1 and type 2 fundamentalists believe in mean reversion. While type 1 chartists and type 1 fundamentalists are always active in the market, type 2 chartists and type 2 fundamentalists are only active when prices are at least a certain distance away from the fundamental value. The speculators' transactions are mediated by a market maker who also adjusts prices with respect to the excess demand.

As it turns out, the dynamics of our model is driven by a piecewise linear map with three separate branches. Formulated in terms of deviations from the fundamental value, the map has the following appearance (see also Figs. 1 and 2). The inner branch of the map, ranging from $-z$ to $+z$ on the x-axis, always has a slope higher than 1 and a positive intercept parameter. The outer two branches have either a slope (i) between 0 and 1 or (ii) between -1 and 0 (and would intersect the origin). It will become apparent below that the dynamics in the inner regime is solely due to the transactions of type 1 speculators, while the dynamics in the outer regimes is due to type 1 and type 2 speculators.

From a mathematical perspective, our results may be outlined as follows. In case (i), only two of the three branches are involved in the asymptotic dynamics. Depending on the intercept parameter, we may have either two coexisting disjoint attractors or only one attractor. If the intercept parameter is relatively high, only one attractor with periodic motion in the generic case (structurally stable) exists, always located in the bull market (and, in exceptional cases, structurally unstable, the attractor is a Cantor set). This regime is completely determined in the parameter space, and we describe the so-called period-adding structure of periodicity regions. If the intercept parameter declines, a second coexisting attractor emerges, always located in the bear market and always chaotic (in k-chaotic intervals, with $k \geq 1$). Case (ii) is much more

Fig. 1 Shape of the map for $P^* > g(-1)$ at $M^1 = 0.2$, $S^1 = 0.75$ and $S^2 = -1.1$
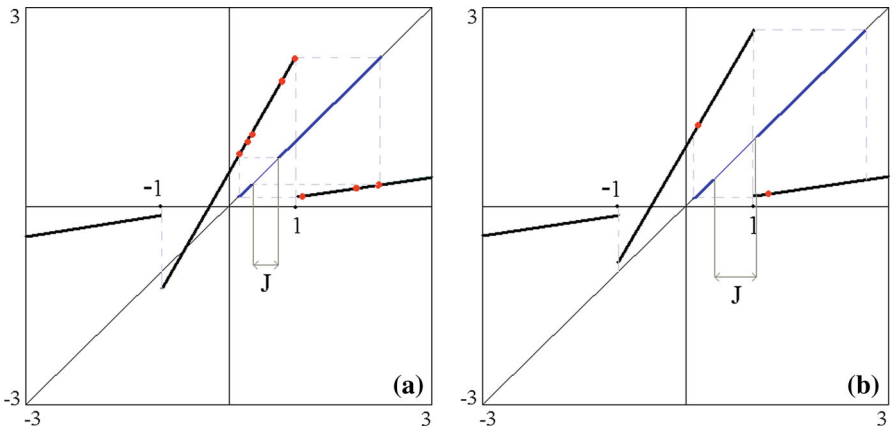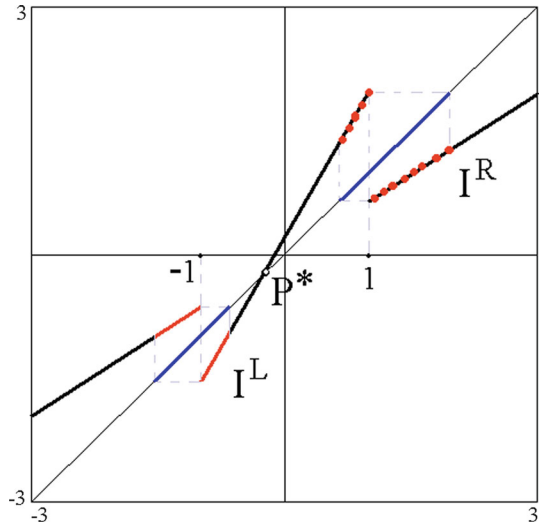

Fig. 2 In **a** shape of the map for $-1 < P^* < g(-1)$ at $M^1 = 0.5$, $S^1 = 0.75$ and $S^2 = -1.6$. In **b** shape of the map when P^* does not exist at $M^1 = 0.9$, $S^1 = 0.75$ and $S^2 = -1.6$

complicated since it may involve all three branches of the map. However, we found that there exist both periodic and chaotic attractors. In a portion of the well-determined parameter space (where the so-called period increment structure exists), the attractors are cycles and there is evidence of bistability, i.e., two periodic cycles may coexist (and be bounded by analytically determined bifurcation curves). What both cases have in common is that the steady state of the model, if it exists, is never stable. Instead, there are either endogenous regular/chaotic dynamics or the system explodes. Contrary to case (i), where the dynamics remains either in the bull or in the bear market, we show that in case (ii) the dynamics switches back and forth between bull and bear markets, and this can occur with both a stable periodicity or in a chaotic way.

It goes without saying that these insights are also relevant from an economic point of view. In addition, we stress here that our model is also capable of generating quite interesting bull and bear market dynamics. Since the model is asymmetric (due to the inner regime's positive intercept parameter), we have, on average, more positive bubbles than negative bubbles, as also seems to be the case for real financial markets. A typical bubble-and-crash path may evolve as follows. First, there is a slow buildup of a bubble. Then the momentum of the bubble process increases—till it crashes. The crash can be quite abrupt and severe. After the crash, the next bubble may start. However, we may also see prices declining for some more time after a crash. Such price reductions sometimes even lead to the aforementioned negative bubbles.

The remainder of our paper is organized as follows. In Sect. 2, we develop our financial market model. In Sect. 3, we report some general properties of our model. Sections 4 and 5 are devoted to an in-depth analysis of our model. In Sect. 6, we conclude the paper.

2 A simple financial market model

The design of our model is highly influenced by those of Day and Huang (1990) and Huang and Day (1993) and may even be regarded as an extension/generalization of their models. The main ingredients of our model may be summarized as follows. We consider a speculative market in which a market maker mediates the transactions of speculators and adjusts prices with respect to the current excess demand: If buying exceeds selling, they increase the price; if selling exceeds buying, they decrease the price. The excess demand is made up of the transactions of four different groups of speculators.

First of all, there are so-called type 1 chartists and type 1 fundamentalists. Type 1 chartists believe in the persistence of bull and bear markets and thus buy if prices are high and sell if they are low. Type 1 fundamentalists do exactly the opposite. Fundamentalists expect prices to return towards their fundamental value and thus buy if prices are low and sell if they are high. Type 1 chartists and type 1 fundamentalists are always active in the market.

By contrast, type 2 chartists and type 2 fundamentalists are not always active. They only become active if the price is at least a certain distance away from its fundamental value. For instance, type 2 chartists may only recognize an exploitable bull/bear market if the misalignment has crossed a certain threshold level. For type 2 fundamentalists, it may only seem reasonable to enter the market as soon as there is some real chance and actual potential for mean reversion. Apart from that, the trading philosophies of type 1 chartists and type 1 fundamentalists are identical to those of type 2 chartists and type 2 fundamentalists.

The dynamics of our model is due to a one-dimensional discontinuous piecewise linear map. In Sect. 2.1, we present the key building blocks of our model. In Sect. 2.2, we derive the model's law of motion. Since the underlying map is very flexible, it cannot be dealt with in just one single paper. Alternatively, sub-classes of models that seem interesting from either a mathematical or economic point of view, or from

both perspectives, should be singled out. A few sub-classes of models, including that which we study in this paper, are introduced in Sect. 2.3.

2.1 The setup

We consider a speculative market in which a market maker mediates the transactions of speculators and adjusts prices with respect to the excess demand. The market maker uses a (standard) log-linear price adjustment rule and quotes the new log price P as

$$P_{t+1} = P_t + a(D_t^{C,1} + D_t^{F,1} + D_t^{C,2} + D_t^{F,2}) \tag{1}$$

Parameter a is a price adjustment parameter. Without loss of generality, we set $a = 1$. The four terms in the bracket on the right-hand side of (1) capture the transactions of type 1 chartists, type 1 fundamentalists, type 2 chartists and type 2 fundamentalists, respectively. Obviously, excess buying drives the price up and excess selling drives it down.

Chartists believe in the persistence of bull and bear markets. We thus formalize the orders placed by type 1 chartists as

$$D_t^{C,1} = \begin{cases} c^{1,a} + c^{1,b}(P_t - F) & \text{if } P_t - F \geq 0 \\ -c^{1,c} + c^{1,d}(P_t - F) & \text{if } P_t - F < 0 \end{cases} \tag{2}$$

The reaction parameters $c^{1,a}$, $c^{1,b}$, $c^{1,c}$ and $c^{1,d}$ are non-negative. Given their beliefs about future price movements, type 1 chartists optimistically buy (pessimistically sell) if prices are in the bull (bear) market, that is, if the log price P is above (below) its log fundamental value F. As usual, the fundamental value is constant and known to all market participants. The reaction parameters $c^{1,a}$ and $c^{1,c}$ capture some general kind of optimism and pessimism, respectively, whereas the reaction parameters $c^{1,b}$ and $c^{1,d}$ indicate how aggressively type 1 chartists trade on their perceived price signals.

Fundamentalists expect prices to return towards their fundamental values. We thus write the orders placed by type 1 fundamentalists as

$$D_t^{F,1} = \begin{cases} -f^{1,a} + f^{1,b}(F - P_t) & \text{if } P_t - F \geq 0 \\ f^{1,c} + f^{1,d}(F - P_t) & \text{if } P_t - F < 0 \end{cases} \tag{3}$$

Again, the reaction parameters $f^{1,a}$, $f^{1,b}$, $f^{1,c}$ and $f^{1,d}$ are nonzero. Hence type 1 fundamentalists always trade in the opposite direction as type 1 chartists. In an overvalued market, they sell and in an undervalued market they buy. Similar to type 1 chartists, the trading intensity of type 1 fundamentalists may depend on market circumstances: A certain mispricing in the bull market may trigger a higher or lower transaction than the same mispricing in the bear market.

Type 2 chartists are only active if prices are at least a certain distance away from their fundamental value. Let $Z > 0$ denote this distance. We can then express the orders placed by type 2 chartists as

$$D_t^{C,2} = \begin{cases} c^{2,a} + c^{2,b}(P_t - F) & \text{if } P_t - F \geq Z \\ 0 & \text{if } -Z < P_t - F < Z \\ -c^{2,c} + c^{2,d}(P_t - F) & \text{if } P_t - F \leq -Z \end{cases} \tag{4}$$

As usual, $c^{2,b}$, $c^{2,d} > 0$, i.e., the trading intensity of type 2 chartists increases with the distance between prices and fundamentals. Moreover, $c^{2,a} \geq -c^{2,b}(Z - F)$ and $c^{2,c} \geq -c^{2,d}(Z + F)$, i.e., the transactions of type 2 chartists are non-negative in the bull market and non-positive in the bear market.

For simplicity, type 2 chartists and type 2 fundamentalists share the same market entry level. We thus model the orders placed by type 2 fundamentalists as

$$D_t^{F,2} = \begin{cases} -f^{2,a} + f^{2,b}(F - P_t) & \text{if } P_t - F \geq Z \\ 0 & \text{if } -Z < P_t - F < Z \\ f^{2,c} + f^{2,d}(F - P_t) & \text{if } P_t - F \leq -Z \end{cases} \tag{5}$$

where the conditions $f^{2,b}$, $f^{2,d} \geq 0$, $f^{2,a} \geq f^{2,b}(F - Z)$ and $f^{2,c} \geq f^{2,d}(F + Z)$ hold. Again, fundamentalists buy if the market is undervalued and sell if it is overvalued.

As we will see in the sequel, assuming common market entry levels for all type 2 agents along with otherwise linear trading rules results in a simple one-dimensional map with two discontinuity points and three linear branches. Our setup allows us to perform a detailed analytical treatment of our financial market model. Given the financial market turmoil we currently face in Europe, we believe that it is important to improve our understanding of financial markets and hope that our paper helps in this respect. Note also that Tramontana and Westerhoff (2013) demonstrate that a stochastic version of our model does quite well in replicating the main stylized facts of financial markets, which may be regarded as empirical support for our approach.

2.2 The model's law of motion

In total, trading rules (2)–(5) contain 16 reaction parameters. To simplify the notation, we introduce the following eight aggregate parameters

$$\begin{cases} m^1 = c^{1,a} - f^{1,a}, & s^1 = c^{1,b} - f^{1,b}, \\ m^2 = f^{1,c} - c^{1,c}, & s^2 = c^{1,d} - f^{1,d}, \\ m^3 = c^{2,a} - f^{2,a}, & s^3 = c^{2,b} - f^{2,b}, \\ m^4 = f^{2,c} - c^{2,c}, & s^4 = c^{2,d} - f^{2,d}. \end{cases} \tag{6}$$

Given the assumptions about the individual reaction parameters, it is clear that each of the eight aggregate parameters can take any value. Furthermore, it is convenient to express the model in terms of deviations from the fundamental value. Defining $\widetilde{P}_t = P_t - F$ and combining (1)–(5), we obtain

$$\widetilde{P}_{t+1} = \begin{cases} m^1 + m^3 + (1 + s^1 + s^3)\widetilde{P}_t & \text{if } \widetilde{P}_t \geq Z \\ m^1 + (1 + s^1)\widetilde{P}_t & \text{if } 0 \leq \widetilde{P}_t < Z \\ m^2 + (1 + s^2)\widetilde{P}_t & \text{if } -Z < \widetilde{P}_t < 0 \\ m^2 + m^4 + (1 + s^2 + s^4)\widetilde{P}_t & \text{if } \widetilde{P}_t \leq -Z \end{cases}, \tag{7}$$

which is a one-dimensional discontinuous piecewise linear map. Since there are no restrictions on the eight aggregate parameters, each of the four branches of (7) can be positioned anywhere in the $(\widetilde{P}_{t+1}, \widetilde{P}_t)$ space. To develop an understanding of the model, it is therefore necessary to study sub-classes of (7).

2.3 Sub-classes of our model

Let us point out a few sub-classes of our model. First, assume that $m^1 = m^2 = m^3 = m^4 = 0$, $s^1 = s^2$ and $s^3 = s^4$. The assumptions concerning the intercept parameters imply the absence of any general kind of optimism or pessimism. The assumptions about the slope parameters imply that the trading intensity of the speculators does not depend on whether the market is in a bull or a bear state. We then have the map

$$\widetilde{P}_{t+1} = \begin{cases} (1 + s^1 + s^3)\widetilde{P}_t & \text{if } \widetilde{P}_t \geq Z \\ (1 + s^1)\widetilde{P}_t & \text{if } -Z < \widetilde{P}_t < Z \\ (1 + s^1 + s^3)\widetilde{P}_t & \text{if } \widetilde{P}_t \leq -Z \end{cases} \tag{8}$$

This map has been studied in detail in Tramontana et al. (2011). While this model cannot produce chaotic dynamics, we found, for instance, that it can produce high-periodicity cycles and quasiperiodic dynamics which have the appearance of being chaotic.

Second, assume again that the speculators react symmetrically to bull and bear market price signals ($s^1 = s^2$ and $s^3 = s^4$). However, the intercept parameters may be nonzero. In the current paper, we consider the case $m^1 = m^2$ and $m^1 = -m^3 = -m^4$. Note that this implies that the general kind of optimism/pessimism of type 1 speculators (exactly) offsets the general kind of optimism/pessimism of type 2 speculators. As a result, we obtain the map

$$\widetilde{P}_{t+1} = \begin{cases} (1 + s^1 + s^3)\widetilde{P}_t & \text{if } \widetilde{P}_t \geq Z \\ m^1 + (1 + s^1)\widetilde{P}_t & \text{if } -Z < \widetilde{P}_t < Z \\ (1 + s^1 + s^3)\widetilde{P}_t & \text{if } \widetilde{P}_t \leq -Z \end{cases} \tag{9}$$

Clearly, the difference between map (8) and map (9) is that the inner branch of map (9) has a nonzero intercept. However, this very simple mathematical difference implies a completely different dynamic behavior. The intrinsic stability with structural instability of the dynamics of map (8) can no longer occur in map (9) with $m^1 \neq 0$: The dense periodic or quasiperiodic trajectories are completely destroyed and substituted by more interesting/realistic dynamic behaviors. Indeed, as we show in Sects. 4 and 5, this new scenario can generate quite interesting dynamic phenomena.

Third, assume that $m^1 = m^2 = 0$, $m^3 = -m^4$, $s^1 = s^2$ and $s^3 = s^4$. We then obtain the map

$$\widetilde{P}_{t+1} = \begin{cases} m^3 + (1 + s^1 + s^3)\widetilde{P}_t & \text{if } \widetilde{P}_t \geq Z \\ (1 + s^1)\widetilde{P}_t & \text{if } -Z < \widetilde{P}_t < Z \\ -m^3 + (1 + s^1 + s^3)\widetilde{P}_t & \text{if } \widetilde{P}_t \leq -Z \end{cases} \tag{10}$$

This map has been studied in Tramontana et al. (2012b). Interestingly, this map embeds the famous model of Huang and Day (1993) as a special case. This is seen when the outer two branches are shifted, via parameter m^3, such that they connect with the inner branch.

Finally, assume that $m^1 = m^2$ and $s^1 = s^2$. The map then turns into

$$\widetilde{P}_{t+1} = \begin{cases} m^1 + m^3 + (1 + s^1 + s^3)\widetilde{P}_t & \text{if } \widetilde{P}_t \geq Z \\ m^1 + (1 + s^1)\widetilde{P}_t & \text{if } -Z < \widetilde{P}_t < Z \\ m^1 + m^4 + (1 + s^1 + s^4)\widetilde{P}_t & \text{if } \widetilde{P}_t \leq -Z \end{cases} \tag{11}$$

In Tramontana and Westerhoff (2013), we studied a stochastic version of this model and found that it can match the stylized facts of financial markets quite well. To be precise, stochastic variations of the model parameters introduce random switches between stability and instability, which can make the dynamics quite unpredictable. This also shows the importance of establishing analytical results about the deterministic skeleton of such maps—they are the key to understanding the dynamics of their stochastic counterparts.

3 Some properties of our model

Let us start our analysis by pointing out some important properties of our model. For ease of exposition, let us now express (9) as

$$F: \quad X' = \begin{cases} (1 + S^1)X + m^1 & \text{if } |X| < Z \\ (1 + S^1 + S^2)X & \text{if } |X| > Z \end{cases} \tag{12}$$

where $S^1 = s^1$ and $S^2 = s^3$. Recall again that parameters S^1, S^2 and m^1 can take positive or negative values, while $Z > 0$.

A first property is that parameter Z is a scale variable. In fact, by using the change of variable $x = X/Z$ and defining the aggregate parameter $M^1 = m^1/Z$, our model in (12) becomes

$$F: \quad x' = \begin{cases} f(x) = (1 + S^1)x + M^1 & \text{if } |x| < 1 \\ g(x) = (1 + S^1 + S^2)x & \text{if } |x| > 1 \end{cases} . \tag{13}$$

to which we shall refer henceforth. Parameter M^1 can be positive, negative or zero. The case $M^1 = 0$ leads to a non-chaotic map with peculiar properties, which has been completely investigated in the paper cited above. The two cases with a positive and

negative sign of M^1 are topologically conjugated to each other, as it can easily be seen using the change of variable $y = -x$. So we can state the following:

Property A *Map F in (13) with $M^1 < 0$ is topologically conjugated with the same map with $M^1 > 0$.*

Thus, in the following, we shall consider only the positive sign, $M^1 > 0$. So the model of interest, which we rewrite as follows:

$$F: \quad x' = \begin{cases} g(x) = (1 + S^1 + S^2)x & \text{if } x < -1 \\ f(x) = (1 + S^1)x + M^1 & \text{if } -1 < x < 1 \\ g(x) = (1 + S^1 + S^2)x & \text{if } x > 1 \end{cases} \tag{14}$$

is represented by a one-dimensional piecewise linear discontinuous map, with two discontinuity points. The study of the dynamics of piecewise linear discontinuous maps with two discontinuity points is a new field of research that is not yet completely understood. An immediate property for our class of maps, associated with the piecewise linear structure, is that the appearance of cycles cannot occur via fold (or tangent) bifurcation, as is usually the case in smooth maps. Instead, here a cycle can only appear/disappear via a *border collision bifurcation*. This term was used for the first time in the papers by Nusse and Yorke (1992, 1995) and is now extensively used in the literature of piecewise smooth systems. A cycle undergoes a border collision bifurcation when one of its periodic points merges with a discontinuity point.

Even if, as we shall see, we can have cycles with periodic points in two or three partitions of the map, only two functions are involved, so that the eigenvalue of a cycle depends only on the number of periodic points in which the functions $f(x)$ and $g(x)$ are applied. Moreover, the flip bifurcations are not the usual ones (we recall that for smooth maps they are associated with the appearance of a stable cycle of double period). In piecewise linear maps, only *degenerate flip bifurcations* can occur, so that at the bifurcation value there exists a whole segment of cycles of double period that are stable but not asymptotically stable. The dynamic effects after the bifurcation are not uniquely defined, and it is possible to have several kinds of dynamics. However, this bifurcation often leads to chaotic sets, i.e., to chaotic intervals (see Sushko and Gardini 2010). Thus, the following property holds (whose proof, as already remarked, is an immediate consequence of the piecewise linear nature of the map):

Property B *A cycle of map F in (13) can appear/disappear only via a degenerate flip bifurcations or a border collision bifurcation. The eigenvalue of a cycle having p periodic points in the middle region ($|x| < 1$) and q outside ($|x| > 1$) is given by $\lambda = (1 + S^1)^p (1 + S^1 + S^2)^q$.*

Moreover, another property is also immediate and excludes cases which are unfeasible in the applied context, since they lead to divergent trajectories. From Property B, we have that when both slopes of the functions $f(x)$ and $g(x)$ are in modulus higher than 1, then all the possible cycles are unstable, as $|\lambda| > 1$. In these cases, a piecewise linear map can only have chaotic dynamics (when bounded trajectories exist) or divergent trajectories. However, due to the particular structure of our map, we have the following property (stating that when all the slopes are in modulus higher than one, then only divergent trajectories can exist):

Property C *Let map F be with* $|1 + S^1| > 1$ *and* $|1 + S^1 + S^2| > 1$, *then any initial condition different from the unstable fixed point (if existent) has a divergent trajectory.*

Depending on the values of the parameters as, for example, positive or negative slopes of functions f and g, we can have different dynamic properties. Thus, it turns out to be suitable to distinguish three cases, depending on the slope of f, as follows: $H_1 : (1 + S^1) > 1$, $H_2 : (1 + S^1) < -1$, and $H_3 : -1 < (1 + S^1) < 1$. In this work, we shall consider the dynamics of the first case, leaving the investigation of the dynamic behaviors in the other cases for further studies. So, let us fix

$$H_1 : (1 + S^1) > 1 \tag{15}$$

and the map as in (14). From Property C, we are led to bounded dynamics for $|1 + S^1 + S^2| < 1$ and can further distinguish between two qualitatively different situations, namely

$$(i) : (1 + S^1) > 1, \ 0 < (1 + S^1 + S^2) < 1 \tag{16}$$
$$(ii) : (1 + S^1) > 1, \ -1 < (1 + S^1 + S^2) < 0 \tag{17}$$

in which the function $g(x)$ defined in the outer branches either increases or decreases.

Before we continue, let us briefly discuss what cases (i) and (ii) imply economically. What both cases have in common is that type 1 chartists trade more aggressively on a given price signal than type 1 fundamentalists (and therefore $s^1 > 0$). Another aspect both cases have in common is that type 1 fundamentalists and type 2 fundamentalists jointly dominate type 1 chartists and type 2 chartists, again with respect to their price-dependent trading intensity. The difference between the two cases is that this dominance is "weak" in case (i) and "strong" in case (ii). Finally, $M^1 > 0$ implies that there is some extra price-independent buying pressure in the inner regime (resulting from fundamentalists in the bear market and chartists in the bull market).

4 Case $M^1 > 0$ and (i)

In this section, we consider assumption (i) on the parameters: $(1 + S^1) > 1$, $0 < (1 + S^1 + S^2) < 1$. As already remarked, we can also fix the sign of parameter M^1, assuming $M^1 > 0$. So the function defined in the middle branch increases with a positive value in $x = 0$, and an unstable fixed point P^*, if existent, belongs to the negative side (as shown in Fig. 1), given by

$$P^* = -M^1/S^1 < 0. \tag{18}$$

Clearly it exists as long as $M^1 < S^1$, as it merges with the discontinuity in $x = -1$ for

$$M^1 = S^1, \tag{19}$$

which thus represents the border collision bifurcation of the fixed point P^*.

In case (i) investigated here, the two discontinuity points of the map may lead to two disjoint absorbing intervals, bounded by the offsets of the functions at the two discontinuity points, inside which the dynamics are different, as shown in Fig. 1.

It is clear (due to $(1 + S^1) > 1$) that the dynamics of the points in the middle branch take only a few iterations to go outside the interval $-1 < x < 1$ where the function $g(x)$ applies, which is contractive by assumption (as $0 < (1 + S^1 + S^2) < 1$). Thus, the orbits are pushed back in the same absorbing interval and cannot diverge. Let us define

$$I^R = [g(1), f(1)] = [(1 + S^1 + S^2), (1 + S^1) + M^1], \tag{20}$$

the absorbing interval on the right-hand side of the origin (which always exists, for $M^1 > 0$), and

$$I^L = [f(-1), g(-1)] = [-(1 + S^1) + M^1, -(1 + S^1 + S^2)], \tag{21}$$

which may be the absorbing interval on the left-hand side of the origin. In fact, this is an absorbing interval as long as $P^* > g(-1)$, i.e., as long as $M^1 < S^1(1 + S^1 + S^2)$. It follows that for

$$0 < M^1 < S^1(1 + S^1 + S^2) \tag{22}$$

we have two coexisting attracting sets in the two disjoint absorbing intervals. Moreover, noticing that the fixed point P^* must exist, as $M^1 < S^1(1 + S^1 + S^2) < S^1$, we have that the basins of attraction are given by $\mathcal{B}(I^R) =]P^*, +\infty[$ (any initial condition in $\mathcal{B}(I^R)$ is mapped in I^R in a finite number of steps, and the trajectory cannot escape from I^R), and by $\mathcal{B}(I^L) =]-\infty, P^*[$ (any initial condition in $\mathcal{B}(I^L)$ is mapped in I^L in a finite number of steps, and the trajectory cannot escape from I^L). Inside the two absorbing intervals, we have different dynamic behaviors, as shown, for example, in Fig. 1: The attracting set is a cycle of period 13 in I^R, while the trajectories are chaotic in the whole interval in I^L.

The restriction of map F to the absorbing I^R is given by

$$F^R : \quad x' = \begin{cases} f(x) = (1 + S^1)x + M^1 & \text{if } x < 1 \\ g(x) = (1 + S^1 + S^2)x & \text{if } x > 1 \end{cases}, \tag{23}$$

while the restriction of F to the absorbing I^L is given by

$$F^L : \quad x' = \begin{cases} g(x) = (1 + S^1 + S^2)x & \text{if } x < -1 \\ f(x) = (1 + S^1)x + M^1 & \text{if } x > -1 \end{cases}. \tag{24}$$

It is clear that a contact bifurcation occurs at $M^1 = S^1(1 + S^1 + S^2)$, leading to the disappearance of the absorbing interval I^L. That is, for $M^1 = S^1(1 + S^1 + S^2)$ any initial condition in $x < 0$, except the fixed point (if existent), is mapped in a finite number of iterations inside the absorbing interval I^R (from which it cannot escape).

Now let us investigate in more detail which kind of dynamics exist inside the absorbing intervals. As immediately verifiable for $M^1 > 0$, we have $g \circ f(1) < f \circ g(1)$, which implies that *the map is uniquely invertible in the absorbing interval* I^R. In fact, from $g \circ f(1) = (1 + S^1 + S^2)[(1 + S^1) + M^1]$ and $f \circ g(1) = (1 + S^1)(1 + S^1 + S^2) + M^1$, we have that the inequality $g \circ f(1) < f \circ g(1)$ holds. Thus, no periodic point can belong to the interval $J = (g \circ f(1), f \circ g(1)) \subset I^R$ (see Fig. 2a,b), as the points belonging to that interval have preimages only external to I^R.

The situation is different in the absorbing interval I^L, where map F^L has the functions $f(x)$ and $g(x)$ with exchanged roles. We have $g \circ f(-1) = (1 + S^1 + S^2)[-(1 + S^1) + M^1]$ and $f \circ g(-1) = -(1 + S^1)(1 + S^1 + S^2) + M^1$, leading to $g \circ f(-1) < f \circ g(-1)$, which implies here that *the map is not uniquely invertible in the absorbing interval I^L* as, in fact, all the points belonging to the interval $(g \circ f(-1), f \circ g(-1)) \subset I^L$ have two distinct rank-one preimages in I^L: one on the right and one on the left of the discontinuity point $x = -1$ (see Fig. 1).

Summarizing, we have proved that the restrictions of map F to the absorbing intervals is a *one-dimensional piecewise linear map with only one discontinuity point and two increasing branches*, which is the kind of map already studied in several papers, such as Keener (1980) and Gardini et al. (2010), where it was proved that, as long as the map is uniquely invertible (resp. non-uniquely invertible) in the absorbing interval, then only regular dynamics (resp. chaotic dynamics) can exist. That is, regular dynamics in the absorbing interval I^R means that either an attracting cycle (of any period) exists, *which is structurally stable* (i.e., the attracting cycles exists for parameter values varying in an interval) or attracting sets with a Cantor structure exist in the interval (but these are *not structurally stable situations:* A small variation of any parameter leads to qualitatively different dynamics, generally a stable cycle). Moreover, bistability cannot occur inside I^R: At each set of values of the parameters, only a unique stable cycle can exist, globally attracting in I^R. Below we shall demonstrate under which conditions suitable cycles exist, showing that all periods can occur, determining a few related periodicity regions.

The occurrence is different in the absorbing interval I^L (as long as this absorbing interval exists) where the map is non-invertible, and the dynamics in I^L can only be chaotic, in a finite number of intervals, with *robust chaos* (following Banerjee et al. 1998) as persistent under parameter variation (see Keener 1980 and Gardini et al. 2010), an example is shown in Fig. 1. Thus, we have proved the following

Theorem 1 *Let map F be as in case $H_1(i)$ with $M^1 > 0$. Then*

(t1) $I^R = [(1 + S^1 + S^2), (1 + S^1) + M^1]$ *is an invariant absorbing interval, inside which a unique stable cycle exists, globally attracting in I^R and structurally stable, or an attractor with Cantor structure exists and is structurally unstable;*

(t2) *for* $0 < M^1 < S^1(1 + S^1 + S^2)$ *the invariant absorbing interval I^R coexists with an invariant absorbing interval $I^L = [-(1 + S^1) + M^1, -(1 + S^1 + S^2)]$, and a robust chaotic attractor exists in I^L, globally attracting in I^L, made up of $k-$chaotic intervals, $k \geq 1$.*

We notice that when the value of M^1 is so high that the unstable fixed point disappears (i.e., $M^1 > S^1$), then only the absorbing interval I^R exists (i.e., part (t1) of
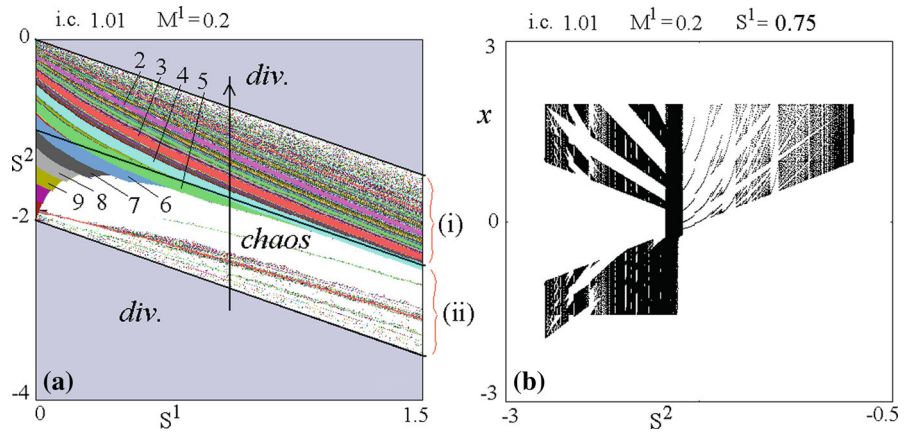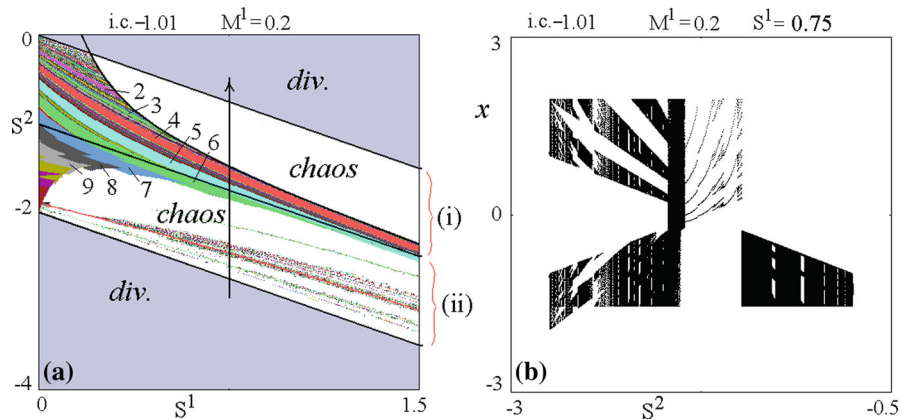
Fig. 3 In **a** the two-dimensional bifurcation diagram illustrates the asymptotic dynamics of an initial condition close to $x = 1$. In strip (*i*) it shows the periodicity regions of attracting cycles belonging to the interval I^R. Different colors correspond to different periods of the cycles. In **b** the one-dimensional bifurcation diagram shows the state variable x as a function of S^2 with S^1 fixed at 0.75 [(along the vertical path shown in (**a**)], and with initial condition close to $x = 1$

Fig. 4 In **a** the two-dimensional bifurcation diagram illustrates the asymptotic dynamics of an initial condition close to $x = -1$. In strip (*i*) the curve separating the chaotic regime in I^L from the periodic regime in I^R has equation $M^1 = S^1(1 + S^1 + S^2)$. In **b** the one-dimensional bifurcation diagram shows the state variable x as a function of S^2 with S^1 fixed at 0.75 [(along the vertical path shown in (**a**)], and with initial condition close to $x = -1$

theorem 1). An example is shown in Fig. 2b, where the attracting set is a stable 2-cycle, globally attracting.

The properties described in the theorem given above are illustrated via the two-dimensional bifurcation diagrams in Figs. 3 and 4. In these figures, we have also evidenced the strips in which the different cases occur, i.e., regions (*i*) and (*ii*) are bounded by straight lines.

The lines of equations $(1 + S^1 + S^2) = 1$ and $(1 + S^1 + S^2) = 0$, that is $S^2 = -S^1$ and $S^2 = -1 - S^1$, bound the region in which case (*i*) occurs. On the other hand,

$(1 + S^1 + S^2) = 0$ and $(1 + S^1 + S^2) = -1$, that is $S^2 = -1 - S^1$ and $S^2 = -2 - S^1$, bound the region in which case (ii) occurs. This yields the regions:

$$
\begin{aligned}
(i) : \quad & S^1 > 0, \ -1 - S^1 < S^2 < -S^1 \\
(ii) : \quad & S^1 > 0, \ -2 - S^1 < S^2 < -1 - S^1.
\end{aligned}
\tag{25}
$$

Now let us complete the analysis of the attracting periodic orbits that can exist in case (i) inside the absorbing interval I^R. As already remarked, the map is topologically conjugated with the piecewise linear map considered in Gardini et al. (2010), so that all the periodicity regions described there associated with the so-called *period-adding structure* can exist. In our case, the discontinuity point is not in the origin, so that either we perform a change of variable or we determine the conditions using our discontinuity point $x = 1$, enabling us to keep the map as given in (23).

We recall that the periodic points may be on the right or left side of $x = 1$, which we denote as the R or L side (where the function $f(x)$ or $g(x)$ is applied, respectively). The cycles are uniquely characterized by a symbolic sequence (cyclically invariant) denoting the sequence of letters of the periodic points of the orbit (and denoting the side to which they belong). To obtain the periodicity regions for the so-called *maximal cycles,* with the symbolic sequence LR^n (having one periodic point on the L side and all the others on the R side), we consider the equation $g^n \circ f(x^*) = x^*$ which gives the periodic point (x^*) of the cycle on the L side. The related cycle exists as long as $g(1) \leq x^* \leq 1$. The equations $x^* = 1$ and $g(1) = x^*$ give the border collision bifurcation curves, leading to the appearance/disappearance of the cycle. We also remark that from the symbolic sequence of the periodic points of a cycle colliding with the discontinuity point $x = 1$, we always immediately have the implicit equation of the border collision bifurcation curves (see Tramontana et al. 2012a). For the cycles with symbolic sequence LR^n, we have $g^n \circ f(1) = 1$, as already remarked (corresponding to the merging $x^* = 1$), and $g^{n-1} \circ f \circ g(1) = 1$ (corresponding to the merging with $x = 1$ of the periodic point close to it from the right).

So, considering that $g^n(x) = (1 + S^1 + S^2)^n x$, the border collision bifurcation curves giving the boundaries of the periodicity regions for cycles with symbolic sequence LR^n of the map F, whose implicit equation is $g^n \circ f(1) = 1$ and $g^{n-1} \circ f \circ g(1) = 1$, are given, respectively, as follows:

$$
(1 + S^1 + S^2)^n (1 + S^1 + M^1) = 1
\tag{26}
$$
$$
(1 + S^1 + S^2)^{n-1} [(1 + S^1)(1 + S^1 + S^2) + M^1] = 1.
\tag{27}
$$

Similarly, to obtain the periodicity regions for the *maximal cycles,* having the symbolic sequence RL^n, we consider the equation $f^n \circ g(x^*) = x^*$, which gives the periodic point on the R side of the cycle. The cycle exists as long as $1 \leq x^* \leq f(1)$. The equations $x^* = 1$ and $f(1) = x^*$ are the border collision bifurcation curves leading to the appearance/disappearance of the cycle. In this case, the collisions of the periodic points of the cycle with the discontinuity $x = 1$ are given by $f^n \circ g(1) = 1$ and $f^{n-1} \circ g \circ f(1) = 1$. Considering that
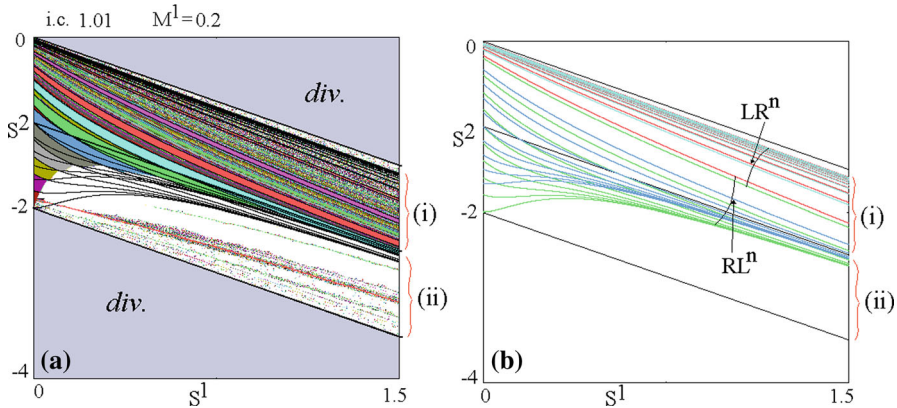
Fig. 5 In **b** we see BCB curves for $n = 1, \dots, 10$ whose equations are given in (26) and (29), in the parameter plane (S^1, S^2) at a fixed value $M^1 = 0.2$. In **a** the curves are drawn above the periodicity regions filled with *different colors*, identifying stable cycles

$$f^n(x) = (1 + S^1)^n x + \frac{(1 + S^1)^n - 1}{S^1} M^1, \qquad (28)$$

we have that the equations of the border collision bifurcation curves giving the boundaries of the periodicity regions for cycles with symbolic sequence RL^n of map F, whose implicit equation is $f^n \circ g(1) = 1$ and $f^{n-1} \circ g \circ f(1) = 1$, are given, respectively, by:

$$(1 + S^1)^n (1 + S^1 + S^2) + \frac{(1 + S^1)^n - 1}{S^1} M^1 = 1 \qquad (29)$$

$$(1 + S^1)^{n-1}(1 + S^1 + S^2)(1 + S^1 + M^1) + \frac{(1 + S^1)^{n-1} - 1}{S^1} M^1 = 1. \qquad (30)$$

In Fig. 5, we have drawn for $n = 1, \dots, 10$ the border collision bifurcation curves whose equations are given in (26)–(27), bounding the family LR^n, and (29)–(30), bounding the family RL^n, in the two-dimensional parameter plane (S^1, S^2) at a fixed value of M^1 ($M^1 = 0.2$). The four different families of curves are shown in color in Fig. 5b and in black in Fig. 5a above the colors identifying regions of stable cycles (the region (ii) will be commented on in the next section). We have also plotted the same curves of families LR^n and RL^n in the parameter plane (S^2, M^1) at a fixed value of S^1 ($S^1 = 0.75$), for $n = 1, \dots, 7$, as shown in Figs. 6 and 7.

Comparing Figs. 6a and 7a numerically obtained with two different initial conditions, one close to $x = 1$ and the other close to $x = -1$, we can see the regions of two coexisting different attracting sets (due to the overlapping of the periodicity regions). In Figs. 6b and 7b, we only show the two families of curves of the first level of complexity (as Leonov 1960a,b called it, see also in Gardini et al. 2010), whose analytical equations have been given above. However, with the adding scheme, infinitely many other periodicity regions can be detected, with the rule that between any two consecutive periodicity regions there are other infinitely many regions associated
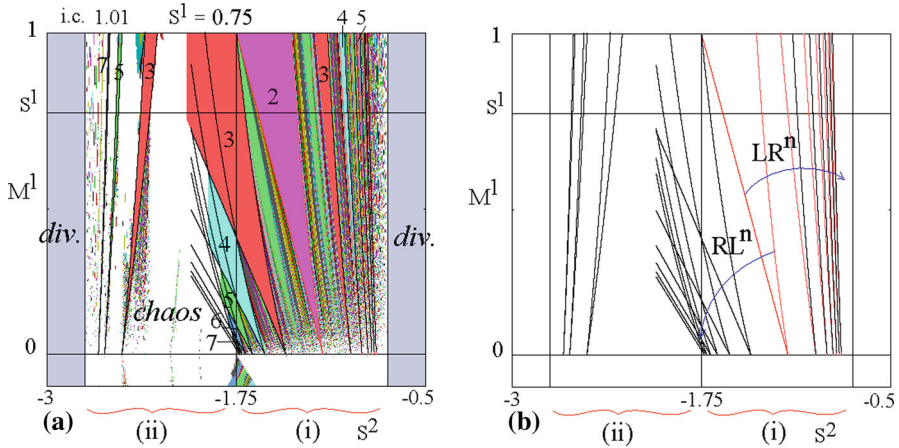
Fig. 6 Parameter plane (S^2, M^1) at $S^1 = 0.75$. In **a** we have periodicity regions with initial condition close to $x = 1$. In **b**, part (i) shows the border collision bifurcation curves of the families LR^n and RL^n for $n = 1, \ldots, 7$; in part (ii) we see the border collision bifurcation curves given in (36) and (37) for $k = 1, 2, 3$
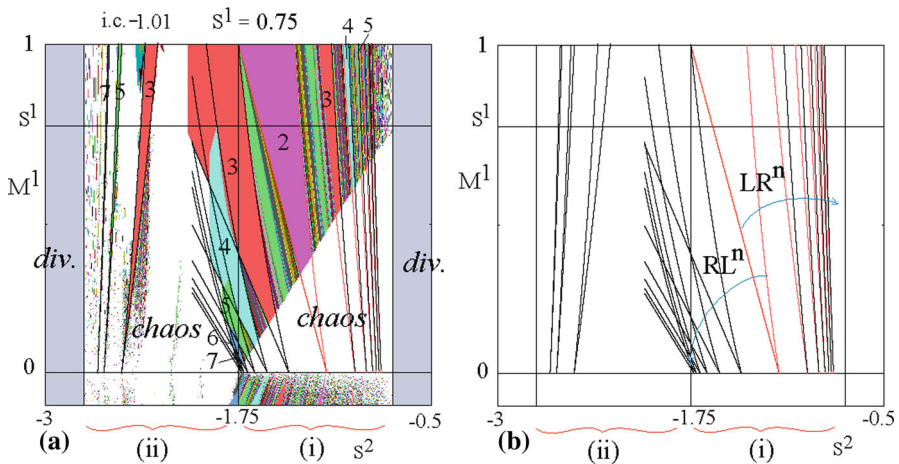

Fig. 7 Parameter plane (S^2, M^1) at $S^1 = 0.75$. In **a** we have periodicity regions with initial condition close to $x = -1$, evidencing the coexistence of different attractors. **b** Reflects the same as in Fig. 6b

with cycles of different periods (following the adding mechanism, and whose rotation numbers follows the Farey summation rule).

We can also analytically obtain the families of border collision bifurcation curves of levels higher than 1, in a method similar to that used for the first level of complexity (the details can be found in Gardini et al. 2010).

Before analyzing of the second case (ii) in the next section, let us close the present one by describing what occurs at the exact bifurcation value between cases (i) and (ii), for $(1 + S^1 + S^2) = 0$, when the external branches are horizontal on the axis. Due to the fact that any trajectory has an iterated point external to the interval $(-1, 1)$ and that outside of this interval the map is set to the value $x = 0$, we have that all the points
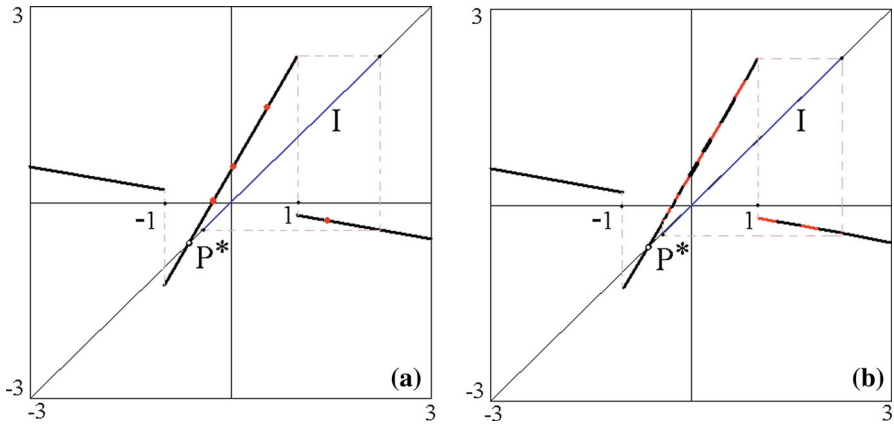
Fig. 8 **a** Attracting 4-cycle at $M^1 = 0.5$, $S^1 = 0.75$ and $S^2 = -1.936$. **b** For $S^2 = -1.937$, soon after the degenerate flip bifurcation, the attracting set is made up of chaotic intervals

have the same asymptotic behavior, which is convergence to a superstable cycle with a periodic point in $x = 0$. The period of the superstable cycle (unique and globally attracting) depends on the parameters' values and can be any integer $n \geq 1$. In Figs. 3, 4 and 5, we can see that the line $(1 + S^1 + S^2) = 0$ crosses several periodicity regions; indeed, all the periods are crossed, as can be seen better in Figs. 6 and 7 (see the vertical line $S^2 = -1.75$), where all the periodicity regions of the family RL^n for $n \geq 1$ (given in (29)) are shown and crossed.

5 Case $M^1 > 0$ and (ii)

Let us now turn to case (ii) for which $-1 < (1 + S^1 + S^2) < 0$. If $g(x)$ has a negative slope, the external branches of our map F are now decreasing, as shown in Fig. 8. Thus, an invariant absorbing interval in the region $x < 0$ cannot exist, as any point $x < -1$ is mapped in the positive side. It follows that in case (ii) there exists a unique invariant absorbing interval I, bounded by the images of the offsets in the discontinuity points, which attracts all the trajectories except, at most, the fixed point.

Consider $g \circ f(1) = (1 + S^1 + S^2)[(1 + S^1) + M^1]$ (which is negative by assumption). Then, we can distinguish the following different ranges for the dynamics:

- (a) for $-1 < P^* < g \circ f(1)$, that is:

$$|1 + S^1 + S^2|(1 + S^1 + M^1) < \frac{M^1}{S^1} < 1, \tag{31}$$

the invariant absorbing interval is given by $I = [g \circ f(1), f(1)] = [(1 + S^1 + S^2)((1 + S^1) + M^1), (1 + S^1) + M^1]$, and the asymptotic dynamics are given by the map $F^R : I \rightarrow I$, as defined in (23);

- (b) for $-1 < g \circ f(1) < P^*$, that is:

$$\frac{M^1}{S^1} < |1 + S^1 + S^2|(1 + S^1 + M^1) < 1, \tag{32}$$

the invariant absorbing interval is given by $I = [f(-1), f(1)] = [-(1 + S^1) + M^1, (1 + S^1) + M^1]$, and the asymptotic dynamics are given by the map defined by three branches, $F : I \rightarrow I$, where F is defined in (14);
- (c) for $g \circ f(1) < -1$, that is:

$$1 < |1 + S^1 + S^2|(1 + S^1 + M^1), \tag{33}$$

the invariant absorbing interval is given by $I = [g \circ f(1), f(1)]$, as in case (a) above, but map F is defined by three branches (as given in (14)), as in case (b) above.

When the parameters satisfy condition (a), then the asymptotic dynamics reduce to that of a discontinuous piecewise linear map with a unique discontinuity point, and branches with slopes of the opposite sign, whose dynamics has been investigated throughly in several papers (Avrutin and Schanz 2006; Avrutin et al. 2006; Gardini and Tramontana 2010). Thus, we know that the dynamics associated with this kind of map either involves stable cycles or chaos. The stable cycles have periodicity regions following the *increment structure* with overlapping, leading to regions of bistability and regions with a unique stable cycle. The chaotic regime occurs with chaos in a unique interval or in $k-$chaotic intervals bounded by the images of the offsets in the discontinuity point.

In our map, we can argue that, close to the bifurcation value $(1 + S^1 + S^2) = 0$, we have the existence of stable cycles. In fact, we can see from Figs. 5, 6 and 7 that one family of periodicity regions exists. These regions are pairwise overlapping. These cycles have the symbolic sequence RL^n for $n \geq 1$, and the boundaries of the related periodicity regions are the border collision bifurcation curves given in (29). The portion of overlapping regions (clearly visible in the figures) corresponds to regions of bistability of the pair of cycles with symbolic sequence RL^n and RL^{n+1}. Inside the existence region of each cycle (bounded by the bifurcation curves given in (29)), the cycle is stable as long as it is on one side of its flip bifurcation curve; on the other side, the cycle exists but is unstable. In fact, as described in Avrutin et al. (2006); Gardini and Tramontana (2010), the stable cycles in this kind of map undergo a flip bifurcation which is, as recalled in section 2, degenerate (see also Sushko and Gardini 2010) and is followed by chaotic dynamics (in chaotic intervals). An example is shown in Fig. 8. Figure 8a shows a unique attracting cycle of period 4, close to its flip bifurcation (the eigenvalue of the cycle in Fig. 8a is given by $(1 + S^1)^3(1 + S^1 + S^2) = -0.9968$). In Fig.8b, we show the chaotic attractor (in chaotic intervals) soon after the degenerate flip bifurcation (occurring when $(1 + S^1)^3(1 + S^1 + S^2) = -1$, i.e., for $S^1 = 0.75$ at $S^2 = -(1 + S^1) - 1/(1 + S^1)^3 = 1.9365889$).
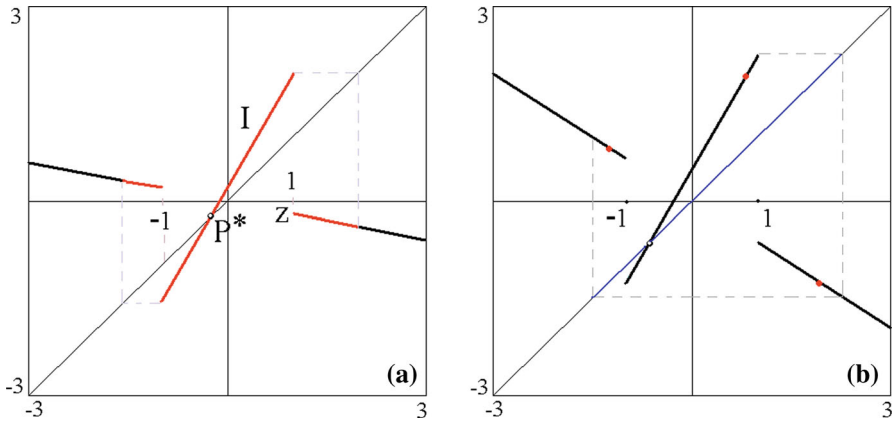
Fig. 9 **a** Chaotic attractor at $M^1 = 0.2$, $S^1 = 0.75$ and $S^2 = -1.95$. **b** Attracting 3-cycle for $M^1 = 0.5$, $S^1 = 0.75$ and $S^2 = -2.4$

Property B yields that the flip bifurcation of the cycle with symbolic sequence RL^n occurs for

$$(1 + S^1)^n(1 + S^1 + S^2) = -1 \tag{34}$$

while that of the cycles with symbolic sequence LR^n occurs for

$$(1 + S^1 + S^2)^n(1 + S^1) = -1. \tag{35}$$

If the parameters satisfy condition (b), we have determined a chaotic regime (an example is shown in Fig. 9a). At the bifurcation value, when $g \circ f(1) = P^*$, the asymptotic dynamics is chaotic in the whole invariant interval I, which is no longer absorbing, having the repelling fixed point on the boundary. The chaotic regime persists, even if we are unable to prove rigorously that stable cycles cannot exist in this regime. Here the map changes its definition, and now three branches are always touched by any trajectory, and the added branch has a slope with a stabilizing effect which, in fact, plays an important role in the other regime (c).

When the parameters satisfy condition (c), although the dominant dynamics are chaotic intervals (always bounded by the images of the endpoints of the absorbing interval I), we can also find regions associated with stable cycles, whose periodic points belong to all three branches of map F. An example is shown in Fig. 9b, where a stable cycle of period 3 (the least period which an orbit in this regime (c) can have) is shown, which is globally attracting. The symbolic sequence of this cycle, in terms of the functions whose composition gives the cycle, is gfg; the region associated with this cycle in the parameter plane corresponding to case (ii) is clearly visible in Figs. 6 and 7. The existence of this kind of cycles is a new phenomenon, associated with the existence of two discontinuity points. In fact, the bifurcations are different to all other border collision bifurcations we have seen so far, in which a cycle appears/disappears due to the collision with a same discontinuity point of two different periodic points

of the cycle (which are the two periodic points closest to discontinuity on opposite sides). Instead, we now have a cycle with periodic points in three different partitions and two discontinuity points, and the appearance/disappearance of the cycle occurs via collision of the periodic points *with two different discontinuities*. In fact, this 3-cycle undergoes its border collision bifurcation when the smallest periodic point merges with $x = -1$ and when the periodic point in the middle region closest to $x = 1$ merges with $x = 1$. The two border collision bifurcation curves associated with its existence are thus given by the implicit equations

$$g \circ f \circ g(-1) = -1 \quad \text{and} \quad g^2 \circ f(1) = 1.$$

Moreover, this is not the only cycle of this kind which can exist and be stable. In fact, other cycles of period $(2k + 1)$ with the symbolic sequence $g^{(2k-1)} fg$ for any $k \geq 1$ can also be stable. In order to detect the border collision bifurcation curves associated with these cycles, we look for the implicit equations

$$g^{2k-1} \circ f \circ g(-1) = -1 \quad \text{and} \quad g^{2k} \circ f(1) = 1.$$

The first equation leads to the border collision bifurcation curves in an explicit form:

$$g^{2k-1} \circ f \circ g(-1) = -1 : \quad M^1 = -\frac{1}{(1 + S^1 + S^2)^{2k-1}} + (1 + S^1)(1 + S^1 + S^2) \tag{36}$$

The second equation (which also corresponds with that already computed above in (26) using $2k$ in place of n) gives:

$$g^{2k} \circ f(1) = 1 : \quad M^1 = \frac{1}{(1 + S^1 + S^2)^{2k}} - (1 + S^1). \tag{37}$$

The bifurcation curves given in (36) and (37) are plotted in the portion (ii) of the parameter plane, for $k = 1, 2, 3$ in Figs. 6 and 7.

Another peculiarity of this new kind of cycle is that they cannot undergo a degenerate flip bifurcation. In fact, by using Property B, we have that their eigenvalue is given by $\lambda = (1 + S^1)(1 + S^1 + S^2)^{2k}$, which is always positive (as $(1 + S^1 + S^2)^2 > 0$), thus a flip bifurcation cannot occur. They can only appear/disappear via border collision bifurcations. If they exist, they are either stable or unstable, depending on the inequality $0 < \lambda < 1$ or $\lambda > 1$, where

$$\lambda < 1 \text{ occurs for } (1 + S^1)(1 + S^1 + S^2)^{2k} < 1.$$

Figure 10a shows the chaotic attractor that exists when the boundary of the border collision bifurcation curve of the stable $3-$cycle in region (ii) is crossed (increasing M^1). Moreover, *we remark that the attracting set here is unique, as two coexisting disjoint attracting sets can occur only in regime (a) described above.*
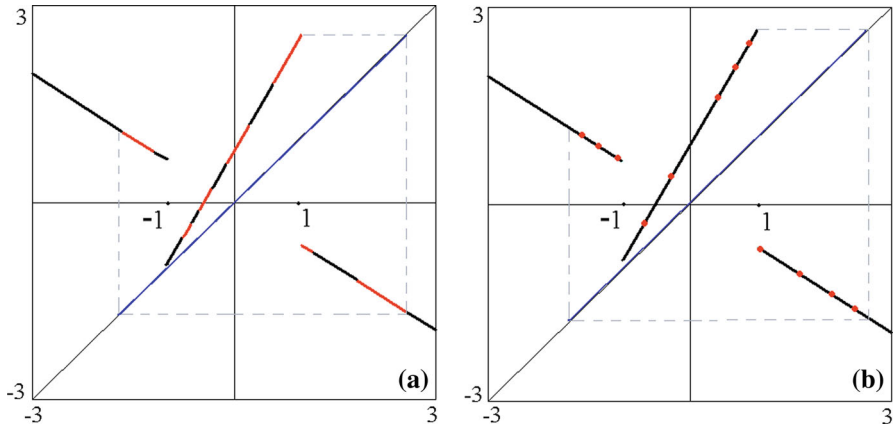
Fig. 10 **a** Chaotic attractor at $M^1 = 0.8$, $S^1 = 0.75$ and $S^2 = -2.4$. **b** Attracting 12-cycle for $M^1 = 0.9$, $S^1 = 0.75$ and $S^2 = -2.4$
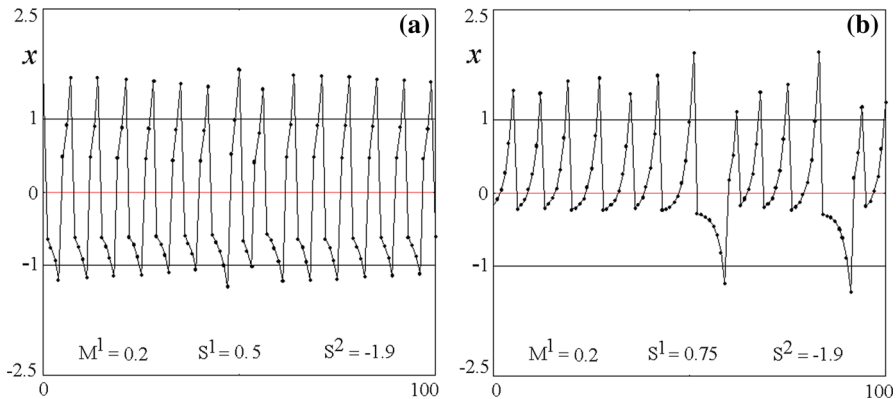

Fig. 11 Versus time trajectory of 100 iterations. **a** At $M^1 = 0.2$, $S^1 = 0.5$ and $S^2 = -1.9$. **b** At $M^1 = 0.2$, $S^1 = 0.75$ and $S^2 = -1.9$

Clearly, the dynamics in this regime (c) are very complicated, and we are far from a complete description of the stable cycles which can exist (due to the interplay of two discontinuity points and thus three branches in the iterated map F). For example, we illustrate in Fig. 10b a stable cycle of period 12, with many periodic points in all three branches, which is not a cycle belonging to the family $g^{(2k-1)}fg$ considered above. And it is possible that several other regions may exist in the parameter space.

Finally, let us explore a few chaotic trajectories belonging to case (*ii*). Of course, the dynamics depicted in Figs. 11 and 12 are only examples. From an economic point of view, however, they are highly interesting. Let us start with the right-hand panel of Fig. 12, where we can see typical bubble-and-crash dynamics. At the beginning, the bubbles slowly buildup. Then the bubble paths accelerate until the movements abruptly crash. Note also that in this panel, there are only positive bubbles, i.e., the temporary price explosion is always upward. In the left-hand panel of Fig. 11, we see
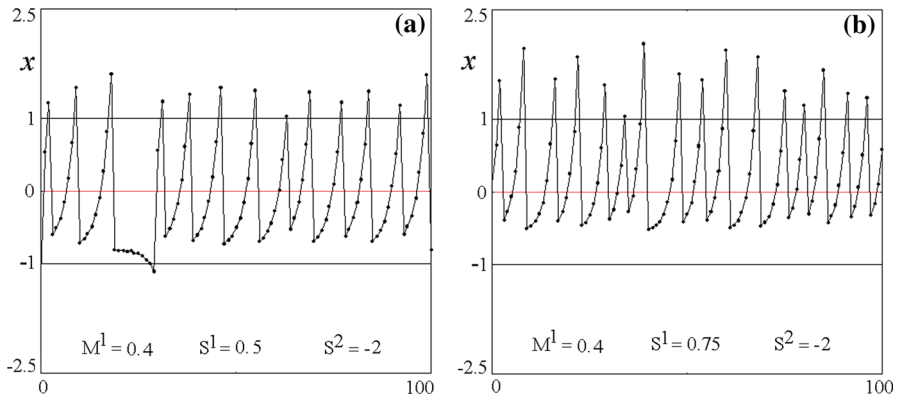
Fig. 12 Versus time trajectory of 100 iterations. **a** At $M^1 = 0.4$, $S^1 = 0.5$ and $S^2 = -2$. **b** At $M^1 = 0.4$, $S^1 = 0.75$ and $S^2 = -2$

a similar picture, with the only exception that now prices decline for longer after a crash. The two other panels (i.e., the right-hand panel of Fig. 11 and the left-hand panel of Fig. 12) reveal that such a further price decline may occasionally even turn into a negative bubble. It goes without saying that all these dynamics mark excess volatility. The fundamental value is constant, and—in an ideal world—prices should thus also be constant and equal to the fundamental value.

In a nutshell, the reasons for the depicted price dynamics are as follows. Since type 1 chartists dominate type 1 fundamentalists, the price dynamics within the inner regime is always unstable. Since there is some additional non-price-dependent buying pressure, prices tend to move upwards and a bubble process is initiated. Once prices enter the region where type 1 chartists and type 2 fundamentalists are active, we have a stronger price correction, i.e., a crash. This pattern repeats itself in a complex manner.

Only now and then do we observe a negative bubble. This may happen when the price-independent buying pressure is overcompensated by the selling orders placed by bearish chartists. Since type 1 chartists become increasingly bearish the lower the price falls, the speed of such a price drop increases. Eventually, however, type 2 speculators become active and then the joint trading behavior of type 1 and type 2 fundamentalists is stronger than the joint trading behavior of type 1 and type 2 chartists. As a result, the negative bubble ends and prices increase, typically quite dramatically, and a positive bubble may start.

6 Conclusions

Financial markets are highly volatile and regularly display significant bubbles and crashes. In this paper, we develop a simple financial market model in the tradition of Day and Huang (1990) and Huang and Day (1993) to improve our understanding of such price movements. Within our model, we consider heterogeneous market participants: a market marker, chartists and fundamentalists. The market maker mediates transactions out of equilibrium and adjusts prices with respect to the excess demand.

Chartist speculators buy assets if prices are high and sell them if they are low—hoping that bull and bear markets persist for longer. Fundamentalist speculators do the opposite: They buy assets if prices are low and sell them if they are high, thus betting on mean reversion. Since some chartists and some fundamentalists only become active if prices are at least a certain distance away from the fundamental value, our model is represented by a discontinuous map.

To be precise, the trading strategies of the speculators imply that the dynamics of the model is driven by a one-dimensional discontinuous piecewise linear map with three branches and two discontinuity points. The inner branch of the map always has a slope higher than one and a positive intercept parameter. The outer two branches have either a slope between zero and one or between minus one and zero. The slopes of the outer two branches are the same, and their intercept parameters are zero. The contribution of this paper is twofold. First, we offer an in-depth mathematical analysis of these kinds of map. Second, we seek to draw lessons from this exercise which may help us improving our understanding of how financial markets function. We find, amongst other things, that the dynamics may involve only two branches of the map or all three of them. In particular, if it involves all three branches, we may see intricate bull and bear market dynamics.

Since our financial market model is rather simple, we can indeed pin down the causalities leading to such price phenomena. The emergence of endogenous bubbles and crashes is obviously a consequence of the trading behavior of the market participants who rely on linear and nonlinear trading strategies. In certain market circumstances, destabilizing chartists dominate the market and their orders tend to drive the price away from the fundamental value. In other market circumstances, however, stabilizing fundamentalists rule the market and prices are pushed toward the fundamental value. As it turns out, these two regimes alternate for a broad range of parameter values in an intricate way, thus generating boom-bust-cycles.

Our model has some straightforward policy implications. A central authority is able change the shape of the map by applying simple linear feedback strategies. For instance, by buying and selling assets proportional to the current mispricing, the central authority renders the slope of the map. Moreover, by buying or selling fixed amounts of assets, it can also alter the position of the map. Therefore, a cleverly designed intervention strategy can guarantee, at least in theory, that the price converges toward its fundamental value (or to any other desired value). Such intervention rules are indeed used by central banks in actual foreign exchange markets. For a financial market application see Westerhoff (2008).

There are several avenues in which our model may be extended. For instance, type 2 chartists and type 2 fundamentalists so far share the same market entry level. Relaxing this simplifying assumption leads to a discontinuous piecewise linear map with five branches and possibly to even more complicated dynamics. One may even consider the case where all agents rely on their own subjective market entry levels. So far, we have only considered a one-dimensional map. By assuming that chartists pay attention to the most recent observed price trend, the model would turn into a two-dimensional map. Note that Sushko and Gardini (2006) present some tools and results for studying higher-dimensional discontinuous maps. However, Tramontana et al. (2009a), Tramontana et al. (2009b) show that certain bifurcation features observed

within a 1D nonlinear (financial market) model carry over to an extended 2D or 3D model version. Another possibility to extend our model is by enriching it with dynamic noise. This could be done by adding additive noise, for instance by allowing for some additional random orders placed by pure noise traders, or by including multiplicative noise, for instance by randomizing the parameter values of the speculators trading rules. It would also be interesting to calibrate or even estimate a stochastic version of our model and to determine in how far it is able to mimic the behavior of actual financial markets. Can it do better than existing models? However, we leave these challenging tasks for the future.

References

Avrutin, V., Schanz, M.: Multi-parametric bifurcations in a scalar piecewise-linear map. Nonlinearity **19**, 531–552 (2006)

Avrutin, V., Schanz, M., Banerjee, S.: Multi-parametric bifurcations in a piecewise-linear discontinuous map. Nonlinearity **19**, 1875–1906 (2006)

Banerjee, S., Yorke, J.A., Grebogi, C.: Robust chaos. Phys. Rev. Lett. **80**, 3049–3052 (1998)

Chiarella, C., Dieci, R., He, X.-Z.: Heterogeneity, market mechanisms, and asset price dynamics. In: Hens, T., Schenk-Hoppé, K.R. (eds.) Handbook of Financial Markets: Dynamics and Evolution, pp. 277–344. North-Holland, Amsterdam (2009)

Day, R., Huang, W.: Bulls, bears and market sheep. J. Econ. Behav. Org. **14**, 299–329 (1990)

Gardini, L., Tramontana, F., Avrutin, V., Schanz, M.: Border collision bifurcations in 1D PWL map and Leonov's approach. Int. J. Bifurcation Chaos **20**(10), 3085–3104 (2010)

Gardini, L., Tramontana, F.: Border collision bifurcations in 1D PWL map with one discontinuity and negative jump. Use of the first return map. Int. J. Bifurcation Chaos **20**(11), 3529–3547 (2010)

Hommes, C., Wagener, F.: Complex evolutionary systems in behavioral finance. In: Hens, T., Schenk-Hoppé, K.R. (eds.) Handbook of Financial Markets: Dynamics and Evolution, pp. 217–276. North-Holland, Amsterdam (2009)

Huang, W., Day, R.: Chaotically switching bear and bull markets: the derivation of stock price distributions from behavioral rules. In: Day, R., Chen, P. (eds.) Nonlinear Dynamics and Evolutionary Economics, pp. 169–182. Oxford University Press, Oxford (1993)

Huang, W., Zheng, H., Chia, W.M.: Financial crisis and interacting heterogeneous agents. J. Econ. Dyn. Control **34**, 1105–1122 (2010)

Keener, J.P.: Chaotic behavior in piecewise continuous difference equations. Trans. Am. Math. Soc. **261**(2), 589–604 (1980)

Leonov, N.N.: On a discontinuous piecewise-linear pointwise mapping of a line into itself. Radiofisika **3**(3), 496–510 (1960a)

Leonov, N.N.: On the theory of a discontinuous mapping of a line into itself. Radiofisika **3**(5), 872–886 (1960b)

Lux, T.: Stochastic behavioural asset-pricing models and the stylize facts. In: Hens, T., Schenk-Hoppé, K.R. (eds.) Handbook of Financial Markets: Dynamics and Evolution, pp. 161–216. North-Holland, Amsterdam (2009)

Nusse, H.E., Yorke, J.A.: Border-collision bifurcations including period two to period three for piecewise smooth systems. Physica D **57**, 39–57 (1992)

Nusse, H.E., Yorke, J.A.: Border-collision bifurcations for piecewise smooth one-dimensional maps. Int. J. Bifurcation Chaos **5**, 189–207 (1995)

Sushko, I., Gardini, L.: Center bifurcation for a two-dimensional piecewise linear map. In: Puu, T., Sushko, I. (eds.) Business Cycle Dynamics: Models and Tools. Springer, Berlin (2006)

Sushko, I., Gardini, L.: Degenerate bifurcations and border collisions in piecewise smooth 1D and 2D maps. Int. J. Bifurcation Chaos **20**(7), 2045–2070 (2010)

Tramontana, F., Gardini, L., Dieci, R., Westerhoff, F.: Global bifurcation in a three dimensional financial model of "bull and bear" interactions. In: Chiarella, C., Bischi, G.I., Gardini, L. (eds.) Nonlinear Dynamics in Economics, Finance and Social Sciences, pp. 333–352. Springer, Berlin (2009a)

Tramontana, F., Gardini, L., Dieci, R., Westerhoff, F.: The emergence of "bull and bear" dynamics in a nonlinear model of interacting markets. Discrete Dynamics in Nature and Society, Vol. **2009**, Article ID 310471 (2009b)

Tramontana, F., Westerhoff, F., Gardini, L.: On the complicated price dynamics of a simple one-dimensional discontinuous financial market model with heterogeneous interacting traders. J. Econ. Behav. Org. **74**, 187–205 (2010)

Tramontana, F., Westerhoff, F., Gardini, L.: A simple financial market model with chartists and fundamentalists: market entry levels and discontinuities. Working Paper (2011)

Tramontana, F., Gardini, L., Avrutin, V., Schanz, M.: New Adding Phenomena in Piecewise Linear Maps with two discontinuities. Int. J. Bifurcation Chaos. **22**, Article ID1250068 (2012a)

Tramontana, F., Gardini, L., Westerhoff, F.: The bull and bear market models of Day and Huang, Some extensions and new results. Working Paper (2012b)

Tramontana, F., Westerhoff, F.: One-dimensional discontinuous piecewise-linear maps and the dynamics of financial markets. In: Bischi, G.I., Chiarella, C., Sushko, I. (eds.) Global Dynamics in Economics and Finance. Essays in Honour of Laura Gardini, pp. 205–222. Springer, Berlin (2013)

Westerhoff, F.: The use of agent-based financial market models to test the effectiveness of regulatory policies. J. Econ. Stat. **228**, 195–227 (2008)

Westerhoff, F.: Exchange rate dynamics: a nonlinear survey. In: Rosser Jr, J.B. (ed.) Handbook of Research on Complexity, pp. 287–325. Edward Elgar, Cheltenham (2009)